



1 Impact of organic acids on chloride depletion of inland 2 transported sea spray aerosols

3 Bojiang Su¹, Zeming Zhuo¹, Yuzhen Fu^{2,3}, Wei Sun^{2,3}, Ying Chen¹, Xubing Du¹,
4 Yuxiang Yang^{2,3}, Si Wu¹, Fugui Huang⁴, Duohong Chen⁵, Lei Li^{1,*}, Guohua Zhang^{2,6},
5 Xinhui Bi^{2,6}, and Zhen Zhou¹

6 ¹ Guangdong Provincial Engineering Research Center for On-line Source Apportionment
7 System of Air Pollution, Institute of Mass Spectrometry and Atmospheric Environment, Jinan
8 University, Guangzhou 510632, PR China

9 ² State Key Laboratory of Organic Geochemistry and Guangdong Key Laboratory of
10 Environmental Protection and Resources Utilization, Guangzhou Institute of Geochemistry,
11 Chinese Academy of Sciences, Guangzhou 510640, PR China

12 ³ University of Chinese Academy of Sciences, Beijing 100039, PR China

13 ⁴ Guangzhou Hexin Analytical Instrument Limited Company, Guangzhou 510530, PR China

14 ⁵ State Environmental Protection Key Laboratory of Regional Air Quality Monitoring,
15 Guangdong Environmental Monitoring Center, Guangzhou 510308, PR China

16 ⁶ Guangdong-Hong Kong-Macao Joint Laboratory for Environmental Pollution and Control,
17 Guangzhou Institute of Geochemistry, Chinese Academy of Sciences, Guangzhou 510640, PR
18 China

19
20 **Correspondence to:* Lei Li (lileishdx@163.com)



21 **Highlights**

- 22 1. Half of the sea salt aerosol (SSA) particles could be assigned as the biological origin.
- 23 2. Organic acids considerably contribute to chloride depletion of SSA particles.
- 24 3. Biological organic coatings may inhibit heterogeneous reactions of SSA particles.



Abstract. Heterogeneous reactions on sea spray aerosols (SSA) are the main pathway to drive the circulation of chlorine, nitrogen, and sulfur in the atmosphere. The release of Cl will significantly affect the physicochemical properties of SSA. However, the impact of organic acids and mixing state on chloride depletion of SSA is still unclear. Hence, the size and chemical composition of individual SSA particles during the East Asian summer monsoon were investigated by a single particle aerosol mass spectrometer (SPAMS). According to the chemical composition, SSA particles were classified into SSA-Aged, SSA-Bio and SSA-Ca. In comparison to the aged Na-rich SSA particles (SSA-Aged), some additional organic species related to biological origin were observed in SSA-Bio, and each of two types accounts for approximately 50% of total SSA particles. SSA-Ca may associated with organic shell of Na-rich SSA particles, which only accounts for ~3%. Strongly positive correlations between Na and organic acids (including formate, acetate, propionate, pyruvate, oxalate, malonate, succinate, and glutarate) were observed for the SSA-Aged ($r^2 = 0.52$, $p < 0.01$) and SSA-Bio ($r^2 = 0.61$, $p < 0.01$), indicating the significance of organic acids in the chloride depletion during inland transport. The contribution of these organic acids to the chloride depletion is estimated to be up to 34%. Interestingly, the degree of chloride depletion is distinctly different between SSA-Aged and SSA-Bio. It is most probably attributed to the associated organic coating in the SSA-Bio particles, which inhibit the displacement reactions between acids and chloride. As revealed from the mixing state of SSA-Bio, Cl / Na ratio increases with increasing phosphate and organic nitrogen, which is known to originate from biological activities. This finding provides some basis for the



47 improvement of modeling simulations in chlorine circulation and a comprehensive

48 understanding of the effects of organics on chloride depletion of SSA particles.

49 **Keywords:**

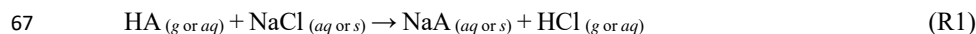
50 Sea spray aerosols; individual particles; chloride depletion; mixing state; organic acids.



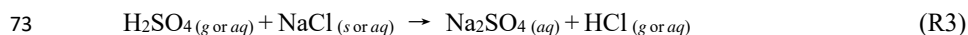
1 Introduction

As one of the largest natural sources of aerosols, sea spray aerosols (SSA) have a global flux of 2000-10000 Tg yr⁻¹ (Gantt and Meskhidze, 2013) and global average distribution of 10.1 µg m⁻² (Ma et al., 2008). SSA are highly complex mixtures, and the chemical composition and mixing state of original SSA depends on the components of local seawater and the mechanisms of formation (Wang et al., 2017). While fresh SSA particles contain approximately 90% sodium chloride (NaCl) in mass, multiphase reactions considerably affect the chemical composition and mixing state, and subsequently, the physical and chemical properties of SSA. The multiphase reactions of SSA, as have been widely reported in field experiments and laboratory studies (Ault et al., 2014; Ghorai et al., 2014; Ryder et al., 2015; Trueblood et al., 2016; Bondy et al., 2017; Martin et al., 2017; Bertram et al., 2018), drive the circulation of elements (e.g., C, O, N, S, P, Cl) affecting tropospheric chemistry and global ecosystem (Finlayson-Pitts, 2003).

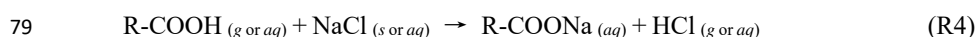
As one of the most important reactions, chloride depletion, as shown in R1, in SSA by interacting with acidic species modifies the physicochemical properties of SSA.



where NaCl represents the major component of SSA, and HA represents acidic species (e.g., HNO₃, H₂SO₄, and organic acids). Generally, inorganic acids are considered as the major contributors to chloride depletion in SSA (Dasgupta et al., 2007; Laskin et al., 2012; Chi et al., 2015), represented as:



However, growing evidence indicates that inorganic acids cannot fully explain the chloride depletion (Laskin et al., 2012). It is therefore proposed that organic acids should be included to further explain the mechanism of chlorine depletion in aged SSA (Ault et al., 2013; Wang and Laskin, 2014; Wang et al., 2015). Similarly, the heterogeneous reactions on SSA with organic acids (R-COOH) can be described as:



(s, solid; aq, aqueous; and g, gaseous)

The physicochemical properties of SSA could be substantially altered through the production of organic salts (Trueblood et al., 2016; Bertram et al., 2018). With ubiquitous existence in the atmosphere, some typical organic acids, such as formic acid, acetic acid, and oxalic acid, may potentially contribute to chloride depletion. Mochida et al. (2003) suggested that organic acids (e.g., oxalic acid and succinic acid) should be considered in the models in order to predict chloride depletion accurately. Through investigating the interactions between the pure NaCl and carboxylic acids in the laboratory, Laskin et al. (2012) even suggested interactions between carboxylic acids and NaCl was the main contribution of chloride depletion. Consistently, Ghorai et al. (2014) observed that some dicarboxylic acids might cause obvious chloride depletion under a specific meteorological condition. These dicarboxylic acids (e.g., malonic acid and succinic acid) are ubiquitous in urban and marine aerosols (Kawamura and Bikkina,



2016), which may come from the polluted continental outflow and the open ocean (Bikkina et al., 2015).

Given the potential contribution of organic acids to the chloride depletion, the understanding of the relative contribution and the influencing factors is still unclear. The investigation of factors that affect chloride depletion is indispensable to understand the ageing process of SSA and the ability to serve as cloud condensation nuclei (CCN) (Drozd et al., 2014; Wang et al., 2015). The morphology of fresh SSA particles is core-shell structure, which consists of salt-core dominated by sodium chloride and outer shell covered by K^+ , Ca^{2+} , Mg^{2+} , SO_4^{2-} , Cl^- and organic components (Laskin et al., 2012; Collins et al., 2014; Chi et al., 2015). These organic components such as alkanes, fatty acids, sugars, dicarboxylic acids and phosphate may emitted from phytoplankton and bacteria in the sea surface microlayer (SSML) (Gaston et al., 2010; Bikkina et al., 2015; Cochran et al., 2017a; Cochran et al., 2017b; Wang et al., 2017), and the chemical composition and size distribution of SSA particles could be greatly changed by wave breaking. In recent literature, organic coatings on the particles resulted from atmospheric oxidation of hydrocarbons of biogenic and anthropogenic origin may significantly regulate uptake of N_2O_5 (Folkers et al., 2003; Ryder et al., 2015).

In the present study, a single particle aerosol mass spectrometer (SPAMS) was used to investigate the particle size, chemical composition and ageing degree of individual SSA particles after long-range inland transport during the summer monsoon, to reveal the relative contribution of organic acids on chloride depletion and the influencing factors. The displacement reactions on the SSA particles with various types



116 of organic acids are considered, and the results suggest a significant impact of organic
117 acids on chloride depletion during inland transport. The influence of biogenic organics
118 in the chloride depletion was also discussed.

119 **2 Materials and Methods**

120 **2.1 Field site description**

121 The sampling site is located at Nanling national background station (Mt. Tianjing,
122 24°41'56" N, 112°53'56" E; 1690 m a.s.l.), which was approximately 350 km north of
123 the South China Sea and 200 km north of the Pearl River Delta (PRD) region. It is also
124 surrounded by a national park forest (273 km²), where there were barely anthropogenic
125 pollutants. However, under the influence of the East Asian summer monsoon, the air
126 mass originated from the South China Sea might cross the PRD region to the sampling
127 site. As can be seen in *Supplement Fig. S1*, four major cluster back trajectories of air
128 masses originated from the South China Sea and Indo China Peninsula transported
129 across inland regions to the sampling site within 72 h. During the sampling period, the
130 average relative humidity was 87%, the average temperature was 26.3°C, the wind
131 direction was mainly southwesterly, and the average wind speed was 10 m s⁻¹. More
132 detailed information on the meteorological data can be found in *Supplement Fig. S2*.

133 **2.2 Instrumentation**

134 Individual particles were analyzed using a SPAMS (Hexin Analytical Instrument
135 Co., Ltd., China) from 11 May to 3 June 2018. The SPAMS was used to on-line measure



the size and chemical composition of individual particles. The design and principles of SPAMS have been reported in detail previously (Li et al., 2011). Briefly, the aerosols are drawn into the aerodynamics lens. Then the collimated particles beam through two continuous laser beams (Nd: YAG laser, 532 nm) with a pace of 6 cm. The obtained time of flight and velocity are corresponding to the vacuum aerodynamic diameter. The velocity of an individual particle is applied to trigger the pulse laser (Nd: YAG laser, 266 nm). Subsequently, the generated ion fragments are detected by a bipolar time-of-flight mass spectrometer. Standard polystyrene latex spheres of 0.2-2.2 μm were used to calibrate vacuum aerodynamic particle sizes (d_{va}) of the measured individual particles.

It is also noted that aerosols were sampled through two parallel inlets. The first one is a ground-based counterflow virtual impactor (GCVI model 1205, Brechtel Manufacturing Inc., USA), sampling the cloud residual particles, dried from cloud droplets (with size larger than 8 μm) during cloud event (i.e., when the relative humidity was higher than 95% and the visibility was lower than 3 km) (Zhang et al., 2017). The other one is a PM_{2.5} sampling inlet, delivering fine particles during cloud free periods.

2.3 Classification of SSA

The general characteristic peaks of SSA particles include m/z 23 [Na]⁺, 39 [K]⁺, 46 [Na₂]⁺, 62 [Na₂O]⁺, 63 [Na₂OH]⁺, 81 [Na₂³⁵Cl]⁺ and 83 [Na₂³⁷Cl]⁺ (Collins et al., 2014; Arndt et al., 2017; Martin et al., 2017). There are some additional organic peaks of biological origin (such as at m/z 58 [C₂H₅NHCH₂]⁺, 59 [N(CH₃)₃]⁺, 74



157 $[(C_2H_5)_2NH_2]^+$, -26 $[CN]^-$, -42 $[CNO]^-$, -63 $[PO_2]^-$, -79 $[PO_3]^-$, etc.), besides sodium-
158 related peaks in SSA particles (Ault et al., 2014; Sultana et al., 2017b). In this study,
159 SSA particles were identified by the presence of peaks at m/z 23, 46, 62, 63, 81 and 83,
160 which was coincident with the previous study at the same site reported by Lin et al.
161 (2019). In addition, these organic signals are also considerable for identification of SSA
162 particles, when the above sodium related peaks exist.

163 A total of ~2 million detected particles were clustered into several groups using an
164 Adaptive Resonance Theory neural network (ART-2a) (Song and Hopke, 1999) with a
165 vigilance factor of 0.75, a learning rate of 0.05 and a maximum of 20 iterations. Based
166 on the above representative peaks, ~50 000 SSA particles were identified. Three types
167 of SSA particles with distinct mass spectral characteristics were obtained, including
168 ~25 000 SSA-Aged, ~25 000 SSA-Bio and 1 500 SSA-Ca, respectively. We note that
169 the mass spectral characteristics of SSA for the cloud residual particles ensemble those
170 for the cloud-free particles. And therefore, we focus on the influence of long-range
171 transport, rather than in-cloud process, on the modification of SSA.

172 3. Results and discussion

173 3.1 General characteristics of inland transported SSA particles

174 Figure 1 provides the averaged positive and negative ion mass spectra of three
175 types of SSA particles. SSA-Aged is characterized by prominent ion signature for m/z
176 at 23 $[Na]^+$, 39 $[K]^+$, 40 $[Ca]^+$, 46 $[Na_2]^+$, 62 $[Na_2O]^+$ and 63 $[Na_2OH]^+$. Some
177 contributions from m/z 24 $[Mg]^+$, 56 $[Fe]^+$ or 56 $[CaO]^+$, 81 $[Na_2^{35}Cl]^+$, 83 $[Na_2^{37}Cl]^+$,



108 $[\text{Na}_2\text{NO}_3]^+$ and 165 $[\text{Na}_2\text{SO}_4]^+$ were also observed. These mass spectral
 characteristics are similar to those in previous literature (Hughes et al., 2000; Collins et
 al., 2014; Sultana et al., 2017a). This type of SSA particles with a significant ion marker
 of Na is typically represented as Na-rich sea salt particles. In the negative ion spectra,
 abundant nitrate were observed due to the ratio of m/z at -46 $[\text{NO}_2]^-$, -62 $[\text{NO}_3]^-$, and -
 147 $[\text{Na}(\text{NO}_3)_2]^-$, in contrast to weak chlorine ion signal at m/z -35 $[\text{Cl}]^-$ and -37 $[\text{Cl}]^-$,
 indicating that the particles have undergone partial but not fully atmospheric ageing
 (Hughes et al., 2000; Sultana et al., 2017b). Several peaks are assigned as organic acids,
 such as formate at m/z -45 $[\text{HCO}_2]^-$, acetate at m/z -59 $[\text{C}_2\text{H}_3\text{O}_2]^-$, propionate at m/z -73
 $[\text{C}_2\text{HO}_3]^-$, pyruvate at m/z -87 $[\text{C}_3\text{H}_3\text{O}_3]^-$, oxalate at m/z -89 $[\text{C}_2\text{HO}_4]^-$, malonate at m/z
 -103 $[\text{C}_3\text{H}_3\text{O}_4]^-$, succinate at m/z -117 $[\text{C}_4\text{H}_5\text{O}_4]^-$, and glutarte at m/z -131 $[\text{C}_5\text{H}_7\text{O}_4]^-$
 (Lin et al., 2019), which may be related to algal activity in the SSML or conversion of
 second organic aerosols (SOAs) in the atmosphere (O'Dowd et al., 2014).

Compared with SSA-Aged, the averaged ion spectra of SSA-Bio are more
 complex. SSA-Bio had significant additional signals from biological organic matter
 (i.e., organic nitrogen and phosphate), besides the general characteristics of the SSA-
 Aged particles (Prather et al., 2013; Guasco et al., 2014). While these markers might
 also be associated with dust (Zawadowicz et al., 2017), it is most likely attributed to
 biological markers herein, since there is negligible ion marker (e.g., Al, Ti, Si) for dust.
 Distinct characteristics of amines (58 $[\text{C}_2\text{H}_5\text{NHCH}_2]^+$, 59 $[\text{N}(\text{CH}_3)_3]^+$) were presented
 in the positive spectra, which is similar to the results in a prior laboratory study (Sultana
 et al., 2017a). Besides, the source of amines could also be influenced by the formation



200 of secondary species (such as animal husbandry and biomass burning) during transport
201 (Cheng et al., 2018). The organic nitrogen (i.e., -26 [CN]⁻, -42 [CNO]⁻) has been
202 assigned to the ionization of amino acids in previous studies (Abneesh et al., 2005;
203 Czerwieniec. et al., 2005). Phosphate peaks at m/z -63 [PO₂]⁻ and -79 [PO₃]⁻ are likely
204 assigned as the ionization of components such as phospholipids in biological cells
205 (Ferguson, 2004; Collins et al., 2013; Cochran et al., 2017a; Cochran et al., 2017b;
206 Nguyen et al., 2017). It is noted that SSA-Bio should be regarded as the SSA population
207 influenced by biological activity (Prather et al., 2013). In addition, the peaks of m/z 56
208 represents [CaO]⁺ / [KOH]⁺ or [⁵⁶Fe]⁺. In contrast to SSA-Aged, those aforementioned
209 organic acids exhibited higher peak signal in SSA-Bio. Similar to SSA-Aged, inorganic
210 acids (-46 [NO₂]⁻, -62 [NO₃]⁻ and -97 [HSO₄]⁻) with strong ion signals were also
211 observed. Despite of the different mass spectral pattern, the behavior and inland
212 transport of SSA-Aged and SSA-Bio may be similar. As can be seen in Fig. S1, the
213 relative proportions of them keep stable in the different air masses. They also exhibit
214 similar size distribution, concentrating in size range of 0.4-0.7 μm and peaking around
215 0.5 μm (Fig. S3).

216 SSA-Ca is identified by relatively higher contributions from calcium-related
217 compounds at m/z 40 [Ca]⁺, 56 [CaO]⁺, 57 [CaOH]⁺, 75 [Ca³⁵Cl₂]⁺, 77 [Ca³⁷Cl₂]⁺, and
218 113 [(CaO)₂H]⁺, whereas associated with smaller sodium peak than other types. The
219 negative spectra are dominated by nitrate, sulfate, organic nitrogen, phosphate and
220 chloride. This SSA population has been previously classified as “organic-carbon-
221 dominated (OC)” (Prather et al., 2013; Collins et al., 2014), likely resulted from the



coating of Na-rich particles through crystallization and precipitation (Sultana et al., 2017a; May et al., 2018). The mass spectral characteristics of the Ca-rich SSA particles are quite similar to those of lake spray aerosols (Axson et al., 2016; May et al., 2018). However, SSA-Ca only accounts for a negligible fraction (3.2%) and thus will not be covered in the following discussions.

3.2 Contribution of organic acids to the chloride depletion in the SSA particles

The linear correlations based on peak area between Na and chloride, sulfate, nitrate, and organic acids in the SSA-Aged and SSA-Bio particles are shown in Fig. 2. As expected, there are strong correlations between Na and nitrate in both the SSA-Aged ($r^2 = 0.79$, $p < 0.01$) and SSA-Bio ($r^2 = 0.86$, $p < 0.01$) particles. In addition, more than 99% of SSA particles are internally mixed with nitrate (Fig. 3). This indicates that chemistry in Reaction 2 (R2) is prevalent during long-range transport (Bondy et al., 2017). This is also consistent with previous studies regarding that nitric acid is a major contributor to chloride depletion (Zhao and Gao, 2008; Chi et al., 2015; AzadiAghdam et al., 2019). It is probably because the concentration of its precursor NO_x ($4.67 \mu\text{g m}^{-3}$) suppresses those of other acids in the south China sector (Wang et al., 2016; Wu et al., 2019).

Strong positive correlations between Na and organic acids are also observed in both the SSA-Aged ($r^2 = 0.52$, $p < 0.01$) and SSA-Bio particles ($r^2 = 0.61$, $p < 0.01$). Furthermore, very high number fractions (NFs) of organic acids are also found in SSA-Aged (72%) and SSA-Bio (59%), as shown in Fig. 3. This indicates the possible



243 presence of organic salts in SSA particles and the substantial contribution of organic
244 acids to the chloride depletion. The detailed mixing state between SSA particles and
245 several detected organic acids, as shown in Fig. S4, indicates that formate, oxalate,
246 malonate, and glutarate are the dominant salts. The relative peak area (RPA) ratio (acids
247 / (sulfate + nitrate + organic acids)) is further applied to roughly evaluate the relative
248 contribution of different acids (nitric acid, sulfuric acid, and organic acids) to the
249 chloride depletion of SSA particles (Fig. S5). In the ageing process of the SSA particles,
250 nitrate occupies a large proportion in the SSA-Aged (63-96%) and SSA-Bio particles
251 (64-95%), respectively. Notably, chloride depletion attributed to organic acids could
252 account for 2–34% in the SSA-Aged particles and 2–29% in the SSA-Bio particles. The
253 relative contribution of organic acids to chloride depletion has been reported to be
254 higher than 30% at the eastern United States coast (Braun et al., 2017) and up to 40%
255 in Southeast Asia (AzadiAghdam et al., 2019). The contribution of sulfuric acids (0-
256 10% versus 0-18 %) is the lowest, although it shows positive correlation ($r^2 = 0.24$, $p <$
257 0.01 versus $r^2 = 0.54$, $p < 0.01$) for the SSA-Aged and SSA-Bio particles, respectively
258 (Fig. 2). In addition, similar variations in peak areas of sulfate, nitrate and organic acids
259 were observed in the SSA-Aged and SSA-Bio particles throughout the sampling period
260 (Fig. S6), indicating a close connection of the formation mechanism between inorganic
261 and organic acids.

262 3.3 Effect of particle type on chloride depletion

263 Cl / Na value is typically applied to evaluate the ageing degree of SSA particles



(Laskin et al., 2012; Bondy et al., 2017). There is a significant difference of Cl / Na between the SSA-Aged (1.9%) and SSA-Bio (5.4%) particles (Fig. 4). This result reflects less chloride remaining in the SSA-Aged, attributed to more severe ageing. It might also be supported by relatively weak positive correlation ($r^2 = 0.46$, $p < 0.01$) between Na and Cl (Fig. 2). This result may be explained by the influence of chemical composition and mixing state on the evolution of the SSA particles (Collins et al., 2014; Quinn et al., 2015; Sultana et al., 2017b). Additionally, concentration calculation was also further quantified the chloride depletion percentage using the following equation:

$$\%Cl^- \text{ depletion} = (1.81 \times [Na^+] - [Cl^-]) / (1.81 \times [Na^+]) \times 100\% \quad (R6)$$

where $[Na^+]$ and $[Cl^-]$ are mass concentrations ($\mu g\ m^{-3}$), and 1.81 is the typical mass ratio of Cl / Na in seawater (Zhao and Gao, 2008; Braun et al., 2017; AzadiAghdam et al., 2019). The overall $\%Cl^-$ for the total SSA particles varying from 55% to 99% with an average of 78% (detailed in *Supplement Table S1*), which is similar to the previous filed study in the PRD region reported by Chen et al. (2016). However, SSA particles are not the only source of chlorine ion in the atmosphere (Lightowlers et al., 1988). The excess $[Cl^-]$ produced by fuel combustion could lower the $\%Cl^-$, which might explain the weak difference between the two assessment methods of ageing degree of SSA particles. Hence, both assessment methods could effectively evaluate the chloride depletion of SSA particles supported by a positive correlation ($r^2 = 0.47$, $p < 0.01$) (Fig. S7).

Further analysis indicates that organic matter of biological origin might play an important role in such inhibition of chloride depletion in the SSA-Bio particles. It is



supported by the relationship between peak area ratio of Cl / Na and the biological origin markers (-26 [CN]⁻, -42 [CNO]⁻, -63 [PO₂]⁻ and -79 [PO₃]⁻) described in section 3.1. As shown in Fig. 5, peak area ratio of Cl / Na exhibits an increasing trend with both phosphate (-63 [PO₂]⁻, -79 [PO₃]⁻) and organic nitrogen (-26 [CN]⁻ and -42 [CNO]⁻). This direct evidence indicated phosphate might have a considerable effect on chloride depletion in SSA particles. The relationship between Cl / Na and organic nitrogen is also consistent with that reported in our previous field observations at the same site (Lin et al., 2019). Previous laboratory study results have also shown that reactivity could be inhibited by the organic matter of biological origin (Ault et al., 2014). As shown in Fig. S8, transmission electron microscopy (TEM) images clearly show NaCl core and organic coating of the SSA particles with various thicknesses. The thicker organic coating may inhibit the reactive uptake of HNO_{3(g)} or N₂O_{5(g)} to SSA particles (Folkers et al., 2003; Ryder et al., 2014; Ryder et al., 2015), resulting in a less released Cl to the atmosphere. Such organic coatings are mostly composed of long-chain hydrocarbon, saccharides, carbohydrate, amine and anionic surfactant (Jayarathne et al., 2016; Bertram et al., 2018), and thus have stronger hydrophobicity and probably inhibit the occurrence of Cl transport of convection and diffusion (Bondy et al., 2017).

4. Conclusion and atmospheric implication

We investigated the chloride depletion of SSA particles after long-range inland transport in south China, during a monsoon season. The SSA particles still account for ~3% of the observed submicron particles and are extensively internally mixed with



307 various acids. While the contribution of nitric acid dominates over other acids to the
308 chloride depletion, our results suggest that the role of organic acids should not be
309 neglected. Up to 34% of chloride depletion could be explained by diverse organic acids.
310 Our results add to the growing body of evidence that carboxylic acid may play a
311 significant role in acid displacement reactions (Ma et al., 2013). Given the substantial
312 influence of organic acids on the hygroscopic properties of SSA (Ghorai et al., 2014),
313 such processes may affect CCN / IN activities and lifetime of SSA (Knopf et al., 2014),
314 and thus should be considered in models to predict the climate impact of SSA accurately.
315 Currently, the calculation model of organic acids (especially water-soluble organic
316 compounds) to chloride depletion is still limited (Laskin et al., 2012; Xu et al., 2013).
317 Peng et al. (2016) suggested organic salts produced by NaCl react with dicarboxylic
318 acids inhibit the volatilization of HCl that is resulting in less chloride depletion. Our
319 data may improve the understanding of chloride depletion responsible for mixing state
320 of diverse organic acids in the future study.

321 In addition, we stress that there is a SSA type (e.g., SSA-Bio) likely attributed to
322 the biogenic origin, exhibiting distinctly different chloride depletion, in comparison
323 with the commonly observed SSA-Aged type. Our data indicate that organic matter of
324 biological origin might play an essential role in such inhibition of chloride depletion in
325 the SSA-Bio particles. As previously reported, the presence of organic coatings on SSA
326 particles could effectively influence the heterogeneous reactivity of SSA particles
327 (Ryder et al., 2015; Bondy et al., 2017). Considering the considerable contribution
328 (~50%) of the SSA-Bio particles to the overall SSA, such information should be useful



329 to improve that model results for the climate impact of SSA.

330

331 **Author contributions**

332 GHZ, LL, and XHB designed the research. BJS, GHZ, and LL analyzed the data,
333 and wrote the manuscript. YZF, XBD, YC, YXY and WS conducted sampling work
334 under the guidance of GHZ, LL, and XHB. DHC had an active role in supporting the
335 sampling work. YZF performed the laboratory analysis of individual particles by
336 TEM/EDS. All authors contributed to the discussions of the results and refinement of
337 the manuscript.

338 **Data availability.** Data are available on request from Lei Li (lileishdx@163.com).

339 **Acknowledgement**

340 This work was supported by the National Nature Science Foundation of China (No.
341 41905106), Guangdong International Science and Technology Cooperation Project
342 (2018A050506020) and Guangdong Foundation for Program of Science and
343 Technology Research (Grant No. 2019B121205006).

344 **Competing interests.** The authors declare that they have no conflict of interest.

345 **References**

346 Abneesh, S. M. E., Pitesky, Paul T, Steele, Herbert J, Tobias, David P, Fergenson, Joanne



347 M, Horn, Scott C, Russell, Gregg A, Czerwieniec, Carlito B, Lebrilla, Eric E,
348 Gard, Matthias, Frank., Maurice E, P., Paul T, S., Herbert J, T., David P, F.,
349 Joanne M, H., Scott C, R., Gregg A, C., Carlito B, L., Eric E, G., and Matthias,
350 F.: Comprehensive Assignment of Mass Spectral Signatures from Individual
351 *Bacillus atrophaeus* Spores in Matrix-Free Laser Desorption/Ionization
352 Bioaerosol Mass Spectrometry, *Anal. Chem.*, 77, 3315-3323,
353 <http://doi.org/10.1021/ac048298p>, 2005.

354 Arndt, J., Sciare, J., Mallet, M., Roberts, G. C., Marchand, N., Sartelet, K., Sellegri, K.,
355 Dulac, F., Healy, R. M., and Wenger, J. C.: Sources and mixing state of
356 summertime background aerosol in the north-western Mediterranean basin,
357 *Atmos. Chem. Phys*, 17, 6975-7001, <http://doi.org/10.5194/acp-17-6975-2017>,
358 2017.

359 Ault, A. P., Moffet, R. C., Baltrusaitis, J., Collins, D. B., Ruppel, M. J., Cuadra-
360 Rodriguez, L. A., Zhao, D. F., Guasco, T. L., Ebben, C. J., Geiger, F. M.,
361 Bertram, T. H., Prather, K. A., and Grassian, V. H.: Size-Dependent Changes
362 in Sea Spray Aerosol Composition and Properties with Different Seawater
363 Conditions, *Environ. Sci. Technol.*, 47, 5603-5612,
364 <http://doi.org/10.1021/es400416g>, 2013.

365 Ault, A. P., Guasco, T. L., Baltrusaitis, J., Ryder, O. S., Trueblood, J. V., Collins, D. B.,
366 Ruppel, M. J., Cuadra-Rodriguez, L. A., Prather, K. A., and Grassian, V. H.:
367 Heterogeneous reactivity of nitric acid with nascent sea spray aerosol: Large
368 differences observed between and within individual particles, *J. Phys. Chem.*



- 369 Lett., 5, 2493-2500, <http://doi.org/10.1021/jz5008802>, 2014.
- 370 Axson, J. L., May, N. W., Colon-Bernal, I. D., Pratt, K. A., and Ault, A. P.: Lake Spray
 371 Aerosol: A Chemical Signature from Individual Ambient Particles, Environ.
 372 Sci. Technol., 50, 9835-9845, <http://doi.org/10.1021/acs.est.6b01661>, 2016.
- 373 AzadiAghdam, M., Braun, R. A., Edwards, E.-L., Bañaga, P. A., Cruz, M. T., Betito,
 374 G., Cambaliza, M. O., Dadashazar, H., Lorenzo, G. R., Ma, L., MacDonald, A.
 375 B., Nguyen, P., Simpas, J. B., Stahl, C., and Sorooshian, A.: On the nature of
 376 sea salt aerosol at a coastal megacity: Insights from Manila, Philippines in
 377 Southeast Asia, Atmos. Environ., 216,
 378 <http://doi.org/10.1016/j.atmosenv.2019.116922>, 2019.
- 379 Bertram, T. H., Cochran, R. E., Grassian, V. H., and Stone, E. A.: Sea spray aerosol
 380 chemical composition: elemental and molecular mimics for laboratory studies
 381 of heterogeneous and multiphase reactions, Chem. Soc. Rev., 47, 2374-2400,
 382 <http://doi.org/10.1039/c7cs00008a>, 2018.
- 383 Bikkina, S., Kawamura, K., and Miyazaki, Y.: Latitudinal distributions of atmospheric
 384 dicarboxylic acids, oxocarboxylic acids, and α -dicarbonyls over the western
 385 North Pacific: Sources and formation pathways, J. Geophys. Res. Atmos., 120,
 386 5010-5035, <http://doi.org/10.1002/2014jd022235>, 2015.
- 387 Bondy, A. L., Wang, B., Laskin, A., Craig, R. L., Nhliziyo, M. V., Bertman, S. B., Pratt,
 388 K. A., Shepson, P. B., and Ault, A. P.: Inland sea spray aerosol transport and
 389 incomplete chloride depletion: Varying degrees of reactive processing
 390 observed during soas, Environ. Sci. Technol., 51, 9533-9542,



- 391 <http://doi.org/10.1021/acs.est.7b02085>, 2017.
- 392 Braun, R. A., Dadashazar, H., MacDonald, A. B., Aldhaif, A. M., Maudlin, L. C.,
 393 Crosbie, E., Aghdam, M. A., Hossein Mardi, A., and Sorooshian, A.: Impact
 394 of Wildfire Emissions on Chloride and Bromide Depletion in Marine Aerosol
 395 Particles, Environ. Sci. Technol., 51, 9013-9021,
 396 <http://doi.org/10.1021/acs.est.7b02039>, 2017.
- 397 Chen, W., Wang, X., Cohen, J. B., Zhou, S., Zhang, Z., Chang, M., and Chan, C.-Y.:
 398 Properties of aerosols and formation mechanisms over southern China during
 399 the monsoon season, Atmos. Chem. Phys., 16, 13271-13289,
 400 <http://doi.org/10.5194/acp-16-13271-2016>, 2016.
- 401 Cheng, C., Huang, Z., Chan, C. K., Chu, Y., Li, M., Zhang, T., Ou, Y., Chen, D., Cheng,
 402 P., Li, L., Gao, W., Huang, Z., Huang, B., Fu, Z., and Zhou, Z.: Characteristics
 403 and mixing state of amine-containing particles at a rural site in the Pearl River
 404 Delta, China, Atmos. Chem. Phys., 18, 9147-9159, [http://doi.org/10.5194/acp-](http://doi.org/10.5194/acp-18-9147-2018)
 405 [18-9147-2018](http://doi.org/10.5194/acp-18-9147-2018), 2018.
- 406 Chi, J. W., Li, W. J., Zhang, D. Z., Zhang, J. C., Lin, Y. T., Shen, X. J., Sun, J. Y., Chen,
 407 J. M., Zhang, X. Y., Zhang, Y. M., and Wang, W. X.: Sea salt aerosols as a
 408 reactive surface for inorganic and organic acidic gases in the Arctic
 409 troposphere, Atmos. Chem. Phys., 15, 11341-11353,
 410 <http://doi.org/10.5194/acp-15-11341-2015>, 2015.
- 411 Cochran, R. E., Laskina, O., Trueblood, J. V., Estillore, A. D., Morris, H. S., Jayarathne,
 412 T., Sultana, C. M., Lee, C., Lin, P., Laskin, J., Laskin, A., Dowling, J. A., Qin,



413 Z., Cappa, C. D., Bertram, T. H., Tivanski, A. V., Stone, E. A., Prather, K. A.,
414 and Grassian, V. H.: Molecular Diversity of Sea Spray Aerosol Particles:
415 Impact of Ocean Biology on Particle Composition and Hygroscopicity, *Chem.*,
416 2, 655-667, <http://doi.org/10.1016/j.chempr.2017.03.007>, 2017a.

417 Cochran, R. E., Ryder, O. S., Grassian, V. H., and Prather, K. A.: Sea Spray Aerosol:
418 The Chemical Link between the Oceans, Atmosphere, and Climate, *Acc. Chem.*
419 *Res.*, 50, 599-604, <http://doi.org/10.1021/acs.accounts.6b00603>, 2017b.

420 Collins, D. B., Ault, A. P., Moffet, R. C., Ruppel, M. J., Cuadra-Rodriguez, L. A.,
421 Guasco, T. L., Corrigan, C. E., Pedler, B. E., Azam, F., Aluwihare, L. I.,
422 Bertram, T. H., Roberts, G. C., Grassian, V. H., and Prather, K. A.: Impact of
423 marine biogeochemistry on the chemical mixing state and cloud forming
424 ability of nascent sea spray aerosol, *J. Geophys. Res. Atmos.*, 118, 8553-8565,
425 <http://doi.org/10.1002/jgrd.50598>, 2013.

426 Collins, D. B., Zhao, D. F., Ruppel, M. J., Laskina, O., Grandquist, J. R., Modini, R. L.,
427 Stokes, M. D., Russell, L. M., Bertram, T. H., Grassian, V. H., Deane, G. B.,
428 and Prather, K. A.: Direct aerosol chemical composition measurements to
429 evaluate the physicochemical differences between controlled sea spray aerosol
430 generation schemes, *Atmos. Meas. Tech.*, 7, 3667-3683,
431 <http://doi.org/10.5194/amt-7-3667-2014>, 2014.

432 Czerwieniec, G. A., Russell, S. C., Tobias, H. J., Pitesky, M. E., Fergenson, D. P.,
433 Steele, P., Srivastava, A., Horn, J. M., Frank, M., Gard, E. E., and Lebrilla,
434 C. B.: Stable Isotope Labeling of Entire *Bacillus atrophaeus* Spores and



- 435 Vegetative Cells Using Bioaerosol Mass Spectrometry, *Anal. Chem.*, 77, 1081-
436 1087, <http://doi.org/10.1021/ac0488098>, 2005.
- 437 Dasgupta, P. K., Campbell, S. W., Al-Horr, R. S., Ullah, S. M. R., Li, J., Amalfitano, C.,
438 and Poor, N. D.: Conversion of sea salt aerosol to NaNO₃ and the production
439 of HCl: Analysis of temporal behavior of aerosol chloride/nitrate and gaseous
440 HCl/HNO₃ concentrations with AIM, *Atmos. Environ.*, 41, 4242-4257,
441 <http://doi.org/10.1016/j.atmosenv.2006.09.054>, 2007.
- 442 Drozd, G., Woo, J., Häkkinen, S. A. K., Nenes, A., and McNeill, V. F.: Inorganic salts
443 interact with oxalic acid in submicron particles to form material with low
444 hygroscopicity and volatility, *Atmos. Chem. Phys.*, 14, 5205-5215,
445 <http://doi.org/10.5194/acp-14-5205-2014>, 2014.
- 446 Fergenson, P. D. M. E. P., Herbert J. Tobias, Paul T. Steele, Gregg A. Czerwieniec, Scott
447 C. Russell, Carlito B. Lebrilla, Joanne M. Horn, Keith R. Coffee, Abneesh
448 Srivastava, Segaran P. Pillai, Meng-Ta Peter Shih, Howard L. Hall, Albert J.
449 Ramponi, John T. Chang, Richard G. Langlois, Pedro L. Estacio, Robert T.
450 Hadley, Matthias Frank, and Eric E. Gard*,.: Reagentless Detection and
451 Classification of Individual Bioaerosol Particles in Seconds, *Anal. Chem.*, 76,
452 373-378, <http://doi.org/10.1021/ac034467e>, 2004.
- 453 Finlayson-Pitts, B. J.: The tropospheric chemistry of sea salt: A molecular-level view
454 of the chemistry of nacl and nabr, *Chem. Rev.*, 103, 4801-4822,
455 <http://doi.org/10.1021/cr020653t>, 2003.
- 456 Folkers, M., Mentel, T. F., and Wahner, A.: Influence of an organic coating on the



457 reactivity of aqueous aerosols probed by the heterogeneous hydrolysis of
458 N₂O₅, *Geophys. Res. Lett.*, 30, <http://doi.org/10.1029/2003gl017168>, 2003.

459 Gantt, B., and Meskhidze, N.: The physical and chemical characteristics of marine
460 primary organic aerosol: a review, *Atmos. Chem. Phys.*, 13, 3979-3996,
461 <http://doi.org/10.5194/acp-13-3979-2013>, 2013.

462 Gaston, C. J., Pratt, K. A., Qin, X. Y., and Prather, K. A.: Real-Time Detection and
463 Mixing State of Methanesulfonate in Single Particles at an Inland Urban
464 Location during a Phytoplankton Bloom, *Environ. Sci. Technol.*, 44, 1566-
465 1572, <http://doi.org/10.1021/es902069d>, 2010.

466 Ghorai, S., Wang, B., Tivanski, A., and Laskin, A.: Hygroscopic properties of internally
467 mixed particles composed of NaCl and water-soluble organic acids, *Environ.*
468 *Sci. Technol.*, 48, 2234-2241, <http://doi.org/10.1021/es404727u>, 2014.

469 Guasco, T. L., Cuadra-Rodriguez, L. A., Pedler, B. E., Ault, A. P., Collins, D. B., Zhao,
470 D. F., Kim, M. J., Ruppel, M. J., Wilson, S. C., Pomeroy, R. S., Grassian, V.
471 H., Azam, F., Bertram, T. H., and Prather, K. A.: Transition Metal Associations
472 with Primary Biological Particles in Sea Spray Aerosol Generated in a Wave
473 Channel, *Environ. Sci. Technol.*, 48, 1324-1333,
474 <http://doi.org/10.1021/es403203d>, 2014.

475 Hughes, L. S., Allen, J. O., Bhawe, P., Kleeman, M. J., Cass, G. R., Liu, D. Y., Fergenson,
476 D. F., Morrical, B. D., and Prather, K. A.: Evolution of atmospheric particles
477 along trajectories crossing the Los Angeles basin, *Environ. Sci. Technol.*, 34,
478 3058-3068, <http://doi.org/10.1021/es9908671>, 2000.



479 Jayarathne, T., Sultana, C. M., Lee, C., Malfatti, F., Cox, J. L., Pendergraft, M. A.,
480 Moore, K. A., Azam, F., Tivanski, A. V., Cappa, C. D., Bertram, T. H., Grassian,
481 V. H., Prather, K. A., and Stone, E. A.: Enrichment of saccharides and divalent
482 cations in sea spray aerosol during two phytoplankton blooms, *Environ. Sci.*
483 *Technol.*, 50, 11511-11520, <http://doi.org/10.1021/acs.est.6b02988>, 2016.

484 Kawamura, K., and Bikkina, S.: A review of dicarboxylic acids and related compounds
485 in atmospheric aerosols: Molecular distributions, sources and transformation,
486 *Atmos. Res.*, 170, 140-160, <http://doi.org/10.1016/j.atmosres.2015.11.018>,
487 2016.

488 Knopf, D. A., Alpert, P. A., Wang, B., O'Brien, R. E., Kelly, S. T., Laskin, A., Gilles,
489 M. K., and Moffet, R. C.: Microspectroscopic imaging and characterization of
490 individually identified ice nucleating particles from a case field study, *J.*
491 *Geophys. Res. Atmos.*, 119, 10,365-310,381,
492 <http://doi.org/10.1002/2014jd021866>, 2014.

493 Laskin, A., Moffet, R. C., Gilles, M. K., Fast, J. D., Zaveri, R. A., Wang, B., Nigge, P.,
494 and Shutthanandan, J.: Tropospheric chemistry of internally mixed sea salt and
495 organic particles: Surprising reactivity of NaCl with weak organic acids, *J.*
496 *Geophys. Res. Atmos.*, 117, n/a-n/a, <http://doi.org/10.1029/2012jd017743>,
497 2012.

498 Li, L., Huang, Z., Dong, J., Li, M., Gao, W., Nian, H., Fu, Z., Zhang, G., Bi, X., Cheng,
499 P., and Zhou, Z.: Real time bipolar time-of-flight mass spectrometer for
500 analyzing single aerosol particles, *Int. J. Mass Spectrom.*, 303, 118-124,



- 501 <http://doi.org/10.1016/j.ijms.2011.01.017>, 2011.
- 502 Lightowlers, P. J., and Cape, J. N.: Sources and fate of atmospheric HCl in the U.K. and
503 western Europe, *Atmos. Environ.*, 22, 7-15, [http://doi.org/10.1016/0004-](http://doi.org/10.1016/0004-6981(88)90294-6)
504 6981(88)90294-6, 1988.
- 505 Lin, Q., Yang, Y., Fu, Y., Zhang, G., Jiang, F., Peng, L., Lian, X., Liu, F., Bi, X., Li, L.,
506 Chen, D., Li, M., Ou, J., Tang, M., Wang, X., Peng, P., and
507 Sheng, G.: Enrichment of submicron sea-salt-containing particles in small
508 cloud droplets based on single-particle mass spectrometry, *Atmos. Chem.*
509 *Phys.*, 19, 10469-10479, <http://doi.org/10.5194/acp-19-10469-2019>, 2019.
- 510 Ma, Q., Ma, J., Liu, C., Lai, C., and He, H.: Laboratory study on the hygroscopic
511 behavior of external and internal C2-C4 dicarboxylic acid-NaCl mixtures,
512 *Environ. Sci. Technol.*, 47, 10381-10388, <http://doi.org/10.1021/es4023267>,
513 2013.
- 514 Ma, X., von Salzen, K., and Li, J.: Modelling sea salt aerosol and its direct and indirect
515 effects on climate, *Atmos. Chem. Phys.*, 8, 1311-1327,
516 <http://doi.org/10.5194/acp-8-1311-2008>, 2008.
- 517 Martin, A. C., Cornwell, G. C., Atwood, S. A., Moore, K. A., Rothfuss, N. E., Taylor,
518 H., DeMott, P. J., Kreidenweis, S. M., Petters, M. D., and Prather, K. A.:
519 Transport of pollution to a remote coastal site during gap flow from California's
520 interior: impacts on aerosol composition, clouds, and radiative balance, *Atmos.*
521 *Chem. Phys.*, 17, 1491-1509, <http://doi.org/10.5194/acp-17-1491-2017>, 2017.
- 522 May, N. W., Gunsch, M. J., Olson, N. E., Bondy, A. L., Kirpes, R. M., Bertman, S. B.,



- 523 China, S., Laskin, A., Hopke, P. K., Ault, A. P., and Pratt, K. A.: Unexpected
524 Contributions of Sea Spray and Lake Spray Aerosol to Inland Particulate
525 Matter, Environ. Sci. Technol., 5, 405-412,
526 <http://doi.org/10.1021/acs.estlett.8b00254>, 2018.
- 527 Mochida, M., Umemoto, N., Kawamura, K., and Uematsu, M.: Bimodal size
528 distribution of C2-C4 dicarboxylic acids in the marine aerosols, J. Geophys.
529 Res. Lett., 30, <http://doi.org/10.1029/2003gl017451>, 2003.
- 530 Nguyen, Q. T., Kjær, K. H., Kling, K. I., Boesen, T., and Bilde, M.: Impact of fatty acid
531 coating on the CCN activity of sea salt particles, Tellus. B., 69,
532 <http://doi.org/10.1080/16000889.2017.1304064>, 2017.
- 533 O'Dowd, C., Ceburnis, D., Ovadnevaite, J., Vaishya, A., Rinaldi, M., and Facchini, M.
534 C.: Do anthropogenic, continental or coastal aerosol sources impact on a
535 marine aerosol signature at Mace Head?, Atmos. Chem. Phys., 14, 10687-
536 10704, <http://doi.org/10.5194/acp-14-10687-2014>, 2014.
- 537 Peng, C., Jing, B., Guo, Y. C., Zhang, Y. H., and Ge, M. F.: Hygroscopic Behavior of
538 Multicomponent Aerosols Involving NaCl and Dicarboxylic Acids, J. Phys.
539 Chem. A, 120, 1029-1038, <http://doi.org/10.1021/acs.jpca.5b09373>, 2016.
- 540 Prather, K. A., Bertram, T. H., Grassian, V. H., Deane, G. B., Stokes, M. D., DeMott, P.
541 J., Aluwihare, L. I., Palenik, B. P., Azam, F., Seinfeld, J. H., Moffet, R. C.,
542 Molina, M. J., Cappa, C. D., Geiger, F. M., Roberts, G. C., Russell, L. M., Ault,
543 A. P., Baltrusaitis, J., Collins, D. B., Corrigan, C. E., Cuadra-Rodriguez, L. A.,
544 Ebben, C. J., Forestieri, S. D., Guasco, T. L., Hersey, S. P., Kim, M. J., Lambert,



- 545 W. F., Modini, R. L., Mui, W., Pedler, B. E., Ruppel, M. J., Ryder, O. S.,
546 Schoepp, N. G., Sullivan, R. C., and Zhao, D. F.: Bringing the ocean into the
547 laboratory to probe the chemical complexity of sea spray aerosol, P. Natl. Acad.
548 Sci. USA., 110, 7550-7555, <http://doi.org/10.1073/pnas.1300262110>, 2013.
- 549 Quinn, P. K., Collins, D. B., Grassian, V. H., Prather, K. A., and Bates, T. S.: Chemistry
550 and related properties of freshly emitted sea spray aerosol, Chem. Rev., 115,
551 4383-4399, <http://doi.org/10.1021/cr500713g>, 2015.
- 552 Ryder, O. S., Ault, A. P., Cahill, J. F., Guasco, T. L., Riedel, T. P., Cuadra-Rodriguez, L.
553 A., Gaston, C. J., Fitzgerald, E., Lee, C., Prather, K. A., and Bertram, T. H.: On
554 the Role of Particle Inorganic Mixing State in the Reactive Uptake of N₂O₅ to
555 Ambient Aerosol Particles, Environ. Sci. Technol., 48, 1618-1627,
556 <http://doi.org/10.1021/es4042622>, 2014.
- 557 Ryder, O. S., Campbell, N. R., Morris, H., Forestieri, S., Ruppel, M. J., Cappa, C.,
558 Tivanski, A., Prather, K., and Bertram, T. H.: Role of organic coatings in
559 regulating n₂o₅ reactive uptake to sea spray aerosol, J. Phys. Chem. A, 119,
560 11683-11692, <http://doi.org/10.1021/acs.jpca.5b08892>, 2015.
- 561 Song, X., and Hopke, P. K.: Classification of single particles analyzed by ATOFMS
562 using an artificial neural network, ART-2A, Anal. Chem., 71, 860-865,
563 <http://doi.org/10.1021/ac9809682>, 1999.
- 564 Sultana, C. M., Al-Mashat, H., and Prather, K. A.: Expanding Single Particle Mass
565 Spectrometer Analyses for the Identification of Microbe Signatures in Sea
566 Spray Aerosol, Anal. Chem., 89, 10162-10170,



- 567 <http://doi.org/10.1021/acs.analchem.7b00933>, 2017a.
- 568 Sultana, C. M., Collins, D. B., and Prather, K. A.: Effect of Structural Heterogeneity in
- 569 Chemical Composition on Online Single-Particle Mass Spectrometry Analysis
- 570 of Sea Spray Aerosol Particles, *Environ. Sci. Technol.*, 51, 3660-3668,
- 571 <http://doi.org/10.1021/acs.est.6b06399>, 2017b.
- 572 Trueblood, J. V., Estillore, A. D., Lee, C., Dowling, J. A., Prather, K. A., and Grassian,
- 573 V. H.: Heterogeneous Chemistry of Lipopolysaccharides with Gas-Phase
- 574 Nitric Acid: Reactive Sites and Reaction Pathways, *J. Phys. Chem. A.*, 120,
- 575 6444-6450, <http://doi.org/10.1021/acs.jpca.6b07023>, 2016.
- 576 Wang, B., and Laskin, A.: Reactions between water-soluble organic acids and nitrates
- 577 in atmospheric aerosols: Recycling of nitric acid and formation of organic salts,
- 578 *J. Geophys. Res. Atmos.*, 119, 3335-3351,
- 579 <http://doi.org/10.1002/2013JD021169>, 2014.
- 580 Wang, B., O'Brien, R. E., Kelly, S. T., Shilling, J. E., Moffet, R. C., Gilles, M. K., and
- 581 Laskin, A.: Reactivity of liquid and semisolid secondary organic carbon with
- 582 chloride and nitrate in atmospheric aerosols, *J. Phys. Chem. A.*, 119, 4498-
- 583 4508, <http://doi.org/10.1021/jp510336q>, 2015.
- 584 Wang, N., Lyu, X. P., Deng, X. J., Guo, H., Deng, T., Li, Y., Yin, C. Q., Li, F., and Wang,
- 585 S. Q.: Assessment of regional air quality resulting from emission control in the
- 586 Pearl River Delta region, southern China, *Sci. Total. Environ.*, 573, 1554-1565,
- 587 <http://doi.org/10.1016/j.scitotenv.2016.09.013>, 2016.
- 588 Wang, X. F., Deane, G. B., Moore, K. A., Ryder, O. S., Stokes, M. D., Beall, C. M.,



- 589 Collins, D. B., Santander, M. V., Burrows, S. M., Sultana, C. M., and Prather,
590 K. A.: The role of jet and film drops in controlling the mixing state of
591 submicron sea spray aerosol particles, *P. Natl. Acad. Sci. USA.*, 114, 6978-
592 6983, <http://doi.org/10.1073/pnas.1702420114>, 2017.
- 593 Wu, Z., Zhang, Y., Zhang, L., Huang, M., Zhong, L., Chen, D., and Wang, X.: Trends
594 of outdoor air pollution and the impact on premature mortality in the Pearl
595 River Delta region of southern China during 2006-2015, *Sci. Total. Environ.*,
596 690, 248-260, <http://doi.org/10.1016/j.scitotenv.2019.06.401>, 2019.
- 597 Xu, G., Gao, Y., Lin, Q., Li, W., and Chen, L.: Characteristics of water-soluble inorganic
598 and organic ions in aerosols over the Southern Ocean and coastal East
599 Antarctica during austral summer, *J. Geophys. Res. Atmos.*, 118, 13,303-
600 313,318, <http://doi.org/10.1002/2013jd019496>, 2013.
- 601 Zawadowicz, M. A., Froyd, K. D., Murphy, D. M., and Cziczo, D. J.: Improved
602 identification of primary biological aerosol particles using single-particle mass
603 spectrometry, *Atmos. Chem. Phys.*, 17, 7193-7212, [http://doi.org/10.5194/acp-](http://doi.org/10.5194/acp-17-7193-2017)
604 17-7193-2017, 2017.
- 605 Zhang, G., Lin, Q., Peng, L., Yang, Y., Fu, Y., Bi, X., Li, M., Chen, D., Chen, J., Cai,
606 Z., Wang, X., Peng, P., Sheng, G., and Zhou, Z.: Insight into the in-cloud
607 formation of oxalate based on in situ measurement by single particle mass
608 spectrometry, *Atmos. Chem. Phys.*, 17, 13891–13901,
609 <https://doi.org/10.5194/acp-17-13891-2017>, 2017.
- 610 Zhao, Y., and Gao, Y.: Acidic species and chloride depletion in coarse aerosol particles

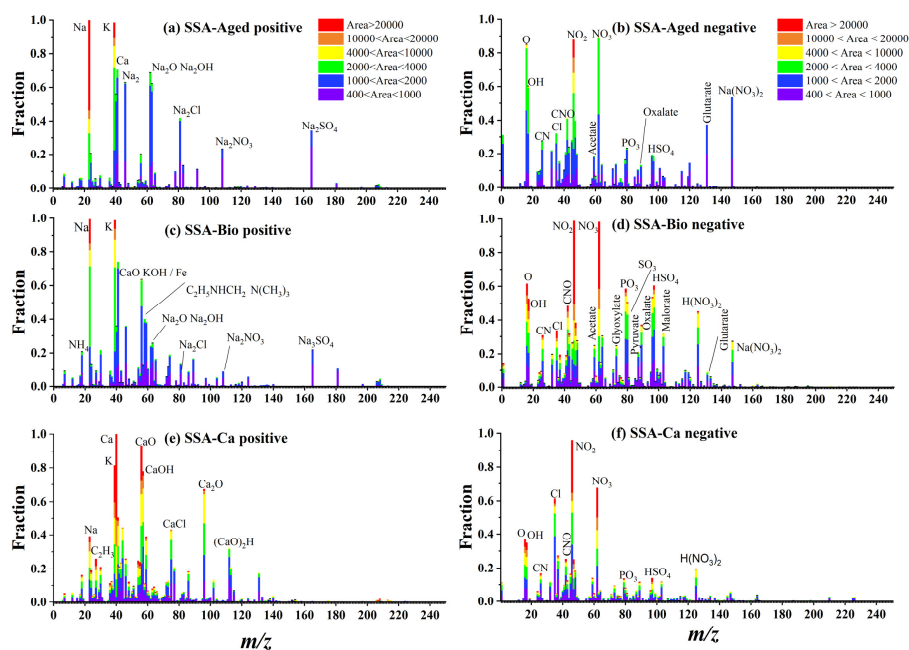


611 in the US east coast, Sci. Total. Environ., 407, 541-547,
612 <http://doi.org/10.1016/j.scitotenv.2008.09.002>, 2008.



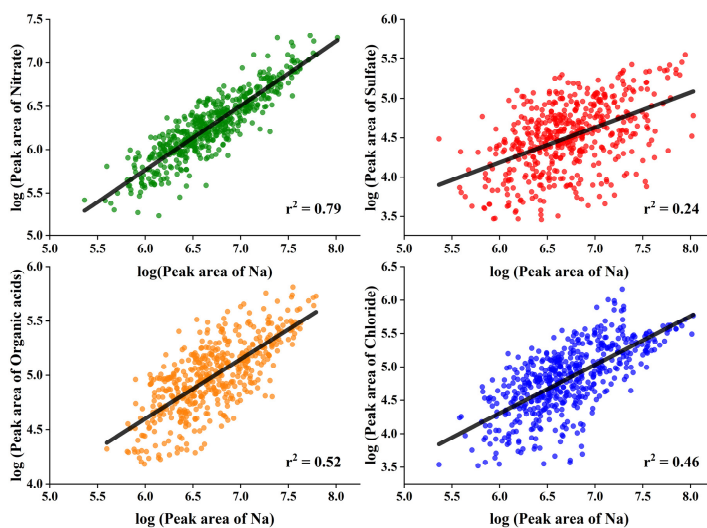
Figures

614

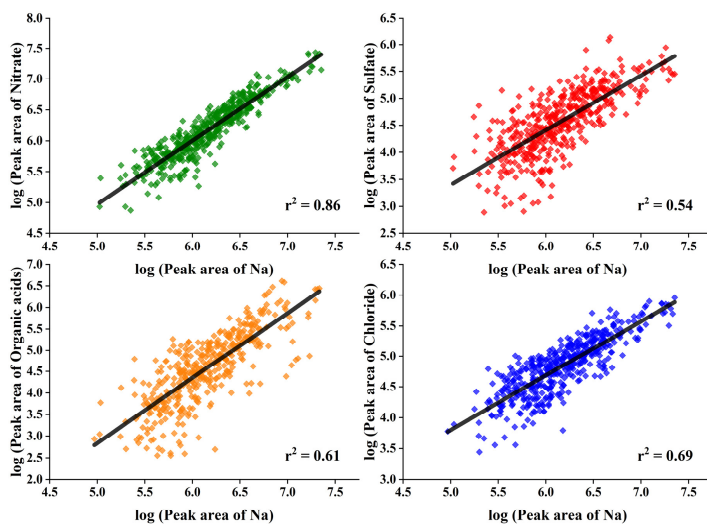


615

616 Figure 1. The averaged digitized positive and negative ion mass spectra of the major
 617 types of SSA particles.

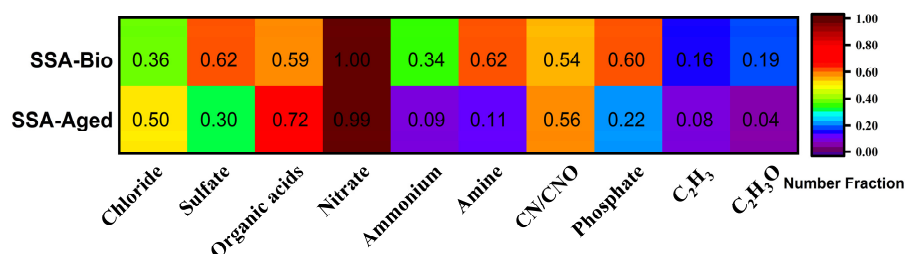


618 (a) SSA-Aged



619 (b) SSA-Bio

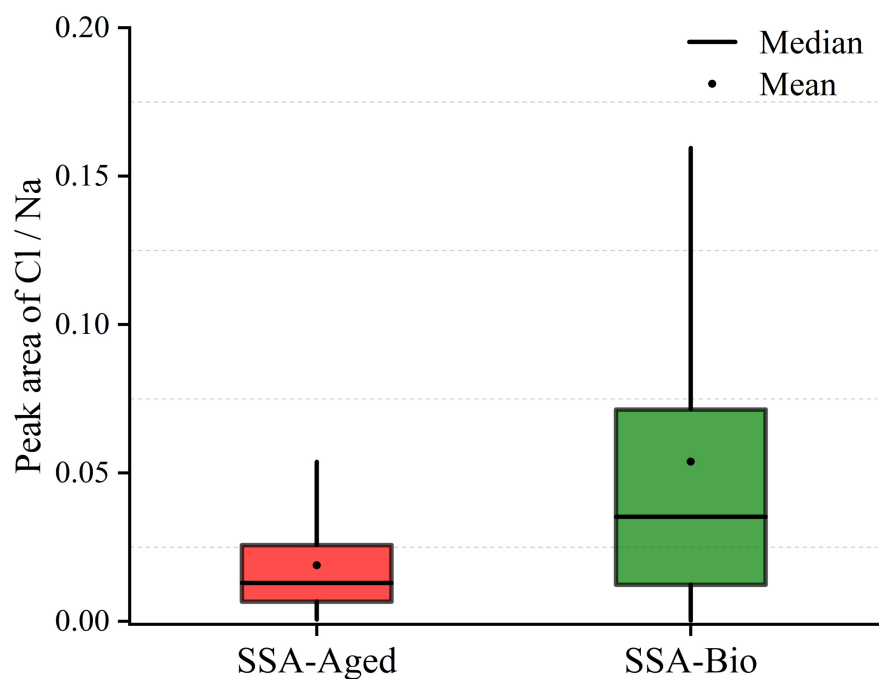
620 Figure 2. Correlations between hourly mean peak area of Na (m/z 23) and sulfate (m/z
 621 -97), nitrate (m/z -46 and 62), organic acids (m/z -45, -59, -73, -87, -89, -103, -117 and
 622 -131) and chloride (m/z -35 and -37) in the SSA-Aged and SSA-Bio. The data is
 623 logarithmically transformed to follow a normal distribution.



624

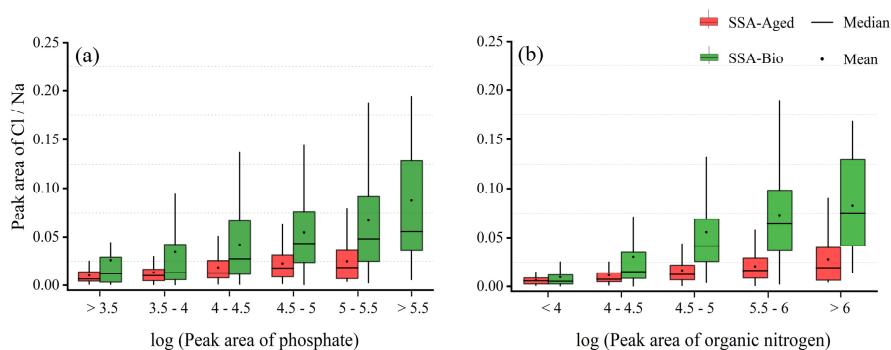
625 Figure 3. Hourly mean number fractions (NFs) of major component in the SSA-Aged
 626 and SSA-Bio. The major component includes chloride (m/z -35 or -37), sulfate (m/z -
 627 97), organic acids (m/z -45, -59, -73, -87, -89, -103, -117 or -131), nitrate (m/z -46 or -
 628 62), ammonium (m/z 18), amine (m/z 58 and 59), organic nitrogen (m/z -26 or -42),
 629 phosphate (m/z -63 or -79), and organic carbon (m/z 27 and 43).

630



631

632 Figure 4. A box and whisker plot of hourly mean peak area of Cl / Na in SSA-Aged
 633 and SSA-Bio. In the box and whisker plot, the lower and upper lines of the box denote
 634 the 25 and 75 percentiles, respectively. The lower and upper edges denote the 10 and
 635 90 percentiles, respectively.



636

637 Figure 5. The logarithmical peak area of phosphate (m/z -63 and -79) and organic
 638 nitrogen (m/z -26 and -42) varied as a function of hourly mean peak area ratio of Cl /
 639 Na.